Recent trend in narrowband sodium lidar and science enabled in the mespause region

Chiao-Yao She
Physics Department, Colorado State University, 200 West Lake Street, Ft. Collins, CO. 80523-1875
(joeshe@lamar.colostate.edu)

Abstract:

In this paper, we describe the salient features of resonance fluorescence and its lidar application to probe the motion of natural occurring Na atoms, from which mesopause region temperature and horizontal wind can be determined on 24-hour continuous basis, weather permitting. A brief history of narrowband Na lidar development as well as its current trend to increase its robustness for remote deployment will be presented. The result of selected Na lidar observations, which reveal the richness of atmospheric waves at different time scales and the effects of their subtle and dramatic interactions in the mesopause region follows.

1. Introduction

The mesopause region (80-110km in altitude) of the earth atmosphere was termed the "ignorosphere" for the lack of observations. Nature also provided us sodium atoms in the mesopause region, and they can be used as tracers for dynamics studies. After its first demonstration [1], laser induced fluorescence (LIF) or resonance scattering from natural occurring Na atoms has been exploited for the observation of mesopause region temperatures in the mid eighties [2] via an excimer pumped dye laser system. A narrowband lidar, utilizing Doppler-free spectroscopy as frequency marker with continuous-wave (cw) single-mode dye laser seeded pulsed dye amplifier (PDA) as transmitter was deployed in Fort Collins, CO (40.6N, 105W). In its first light in August 1989 the lidar observed nocturnal temperatures and associated waves [3]. This lidar has been upgrades for Doppler wind measurements in 1994 [4] and daytime observation using a novel Faraday filter in 1996 [5]. Since May, 2002, the Colorado State University (CSU) Na lidar has been operated regularly for simultaneous observation of mesopause region temperature, zonal and meridional winds as well as Na density on 24-hour continuous basis, weather permitting. Like other lidar systems, the CSU Na-lidar system consists of a transmitter and a receiver. The transmitter starts from a single-mode ring dye laser pumped by a continuous-wave (cw) YAG laser. The cw dye laser is frequency locked to the sharpest Lamb dip, ν_a, in the Na D_2 Doppler-free spectrum [6] as monitored by a laboratory setup. The cw beam is then sent through a dual-pass acousto-optic modulator (AOM) to cyclically shift its frequency up and down by 630 MHz to ν_+ and ν_-, within the Doppler-broadened width of the Na D_2 transition at 589.16 nm. The cw laser beam of ~ 100 mW at the 3 frequencies is then used as the seed beam for the PDA, whose output with megawatt power is sent up to the atmosphere for lidar observation. The locking accuracy of the cw dye laser is 1-2 MHz, giving a line-of-wind accuracy of 1 – 1.5 m/s. The lidar has two beams; one pointing east, the other pointing north (both tilted 30º from zenith). Aligned to each channel is a 14" telescopes for collecting the back scattered signal, which after passing through a narrowband interference filter (~3nm FWHM) and a ultra-narrow Faraday Filter with 2 GHz, FWHM (only for observation under sunlit condition to reject sky background), is sent onto a photomultiplier tube followed by photon-counting electronics. The returned LIF signal sorted by time-of-flight displays a photocount profile. By measuring the altitude-resolved relative LIF of Na backscattered signals at the 3 frequencies, we determine Doppler broadening and shift in fluorescence emission, thereby mesopause region temperature and line-of-sight wind.

With the CSU system as a basic configuration, we deployed a similar system to Artic Lidar Observatory for Middle Atmosphere Research (ALOMAR), with a developing solid-state sum-frequency-generator (SFG) [7] replacing the single-mode cw dye laser. The development towards all-solid-state transmitter then leads to a proposed mobile Na lidar. This paper will summarize these developments as well as atmospheric sciences in the mesopause region enabled by Na lidar observations at both CSU and ALOMAR.

2. Salient features of a narrowband Na lidar

The main advantage of resonance scattering and LIF over Rayleigh scattering lies in the fact that its cross section could be 15 orders of magnitude higher. In the mesopause region, the air density is about 10 orders of magnitude higher than Na density, the returned LIF signal is still 5 orders stronger. Since the lidar return signal is proportion to transmitter power (P), receiver area (A), concentration of scatterers (or mixing ratio, M) and scattering cross section (S) relative to Rayleigh scattering (or PAMS), the advantage of LIF over Rayleigh scattering can be more clearly revealed by considering the PAMS product instead of the usual power-aperture (PA) product of a lidar [8].

In Table 1, we compare the PAMS product between a 20 W Rayleigh lidar at 532 nm with a 3.5-m diameter telescope and a 0.5 W Na lidar at 589 nm with a 35-cm

telescope, both operating at 90 km. Though the PA product of the former is 4000 times higher, its PAMS product is about 15 times lower. As a result, The LIF signal of a Na lidar at 90 km, is comparable to the Rayleigh signal at 25 km (see Fig. 2).

Table 1 PA vs. PAMS for Rayleigh and Na lidars

Definition of parameters	Rayleigh lidar 3.5-m	Sodium lidar 35-cm
Power (Watt)	20	0.5
Area (m^2)	10	0.1
Mixing ratio of species (90 km)	1	$5.2x10^{-11}$
Sigma in the unit of $6x10^{-32}$ m^2/sr	1	$1.25x10^{15}$
Wavelength (nm)	532	589
PA (Wm^2)	200	0.05
PAMS (Wm^2)	200	3120

In order to take the advantage of resonance scattering, the absolute frequency of the transmitting laser must be known to within 1 - 2 MHz. It is therefore fortunate that we have Doppler-free spectrum as an absolute frequency marker, whose features are not affected by ambient temperature, a property highly desirable for multi-day continuous operation. The Doppler-free spectrum of the Na D_2 transition is shown in Fig. 1, with the frequency scale referenced to the center of the Na D_2 transition. The selected 3 frequencies for lidar operation are ν_a = -651.4 MHz, ν_+ = -21.4 MHz, and ν_- = -1,281.4 MHz, which were determined to within 0.1 MHz accuracy via laboratory experimentation, However, the laser frequency can only be locked to within 1 – 2 MHz in real time.

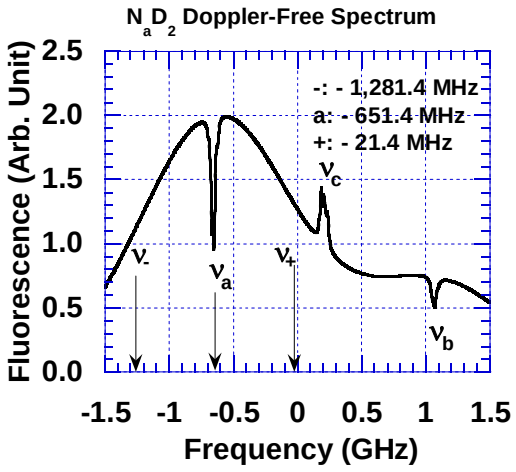

Figure 1 Doppler-free spectrum used to lock the laser at ν_a, which is shifted cyclically to ν_+ and ν_- by AOM

The effectiveness of Faraday filter in daytime sky background rejection can be seen when the received photon profiles between local noon and night are compared. Figure 2 shows three 2-min photon files at ν_a taken at different times of the day. The black profile was taken during day break. The blue file was taken 13 min later, still under nighttime condition but with the Faraday filter inserted. Though the signal is lower by about a factor of five, the background is reduced by a factor of 6000 to 8000, giving the blue profile a higher signal to noise ratio. The orange profile was taken around local noon; its signal is comparable to the blue profile, and the background, while much higher than that of the blue file, is only about a factor of 2 higher than the nighttime background without the Faraday filter. That the Na signal can be seen at noon with 2-min integration using a small telescope is a testimony to the effectiveness of the Faraday filter.

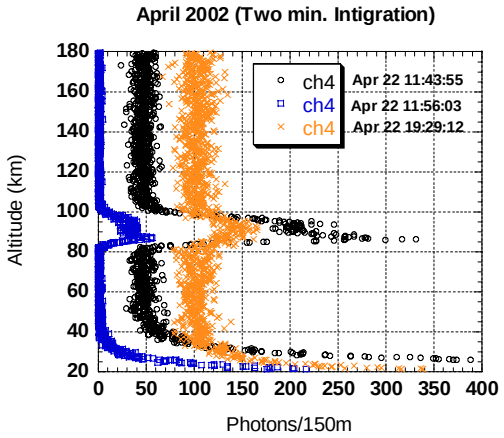

Figure 2 Lidar profiles at night with (blue) and without (black) and noon with (orange) Faraday filter.

3. Recent trend in Na lidar upgrades

Nature provided us Na density and fluorescence cross section, they can not be changed. The only way to increase Na lidar signal is then to increase transmitter power and/or receiver area, as well as to reduce background noise. Since it is not practical to increase the transmitter power at 589 nm, nor is it desirable to do so to avoid saturation of the Na layer. One obvious way to increase the signal is to use a large telescope, which is costly, or multiple telescopes. We therefore, in collaboration with Colorado Research Associates, deployed a somewhat different narrowband Na lidar to ALOMAR inside the Norwegian arctic to take the advantage of the 1.8-m twin telescope there [9]. With the same transmitter power, this increases the signal level by 25 times over the lidar at CSU. Other distinct motivation for going to ALOMAR is its Arctic location, which provided extremely cold summer mesopause and its accompanying often dramatic dynamics. Though Na Faraday filter has performed wonders under sunlit

conditions, to find a cleaver way to recover the 50% signal lost and to make it more robust in operation is an area of continued research.

Since the Na lidar at CSU uses two dye laser systems, one of which (PDA) requires dye change after every 24 hours of operation. This leads to a loss of 10 – 20 minutes in observation time per day. A dye system in general is not desirable, especially for remote deployment. For the ALOMAR system, we got rid of the cw ring dye laser and uses SFG to produce cw Na light at 589 nm. This light is generated from a miniature (1 cm long) nonlinear resonator of single crystal $LiNbO_3$ pumped by light beams from two c.w. monolithic Yag lasers, at 1064 nm and at 1319 nm. For efficient conversion, the $LiNbO_3$ resonator is kept at the SFG phase matching temperature of ~ 224 ^oC, and its surface coated with multi-layer films. Due to its self contained electronics for tuning and Doppler-free locking to ν_a, this system has the potential for remote and automatic operation. Though initially, the e-beam coating on resonator surface was problematic, the current resonator with resilient ion-beam-sputtered coating allowed continuous SFG operation since 2004.

For future deployment in narrowband Na lidar, one looks for the use multiple telescopes to achieve large equivalent receiver area, and to provide versatile deployment for different science goals with at least two distinct beams. More challenging is the development of all-solid-state transmitter for robust and remote deployment. One such system under consideration is to adapt the proven solid-state system, which had deployed to remote location for mesopause temperature observations [10], and convert it to a system capable of measuring both temperatures and winds [11]. The temperature-only system used pulsed sum-frequency generation of 589 nm light from a nonlinear crystal pumped by two pulsed Yag lasers, one at 1064 nm and the other at 1319 nm. Our proposal in addition introduces a simpler low-power cw SFG at 589 nm [12] as a frequency marker to guide the tuning of the infrared seeding light to the power pulsed lasers. With the use of AOM to shift the frequency of seeding light by an appropriate amount, we can cyclically produce 3 selected frequencies with an all-solid-state transmitter for remote deployment. The same Faraday filter can be used for observation under sunlit conditions. Further, the cw SFG light has enough tuning range for the characterization of Faraday filter transmission, required from time to time as practiced with the CSU system.

4. Science in the mesopause enabled by the Na lidar

To illustrate the power of a narrowband Na lidar for science studies in the mesopause region, we present two teasing examples here. The longest lidar campaign occurred at Fort Collins in September 2003. It is a 14-day campaign with a 9-day continuous observation of mesopause region temperature (T), zonal (U) and meridional (V) winds. We have computed the simultaneous TUV profiles with 2-km_15-min and 4-km_30-min resolution, respectively, for observations at night and under sunlit conditions. The TUV contour plots of the 9-day continuous run are shown in Fig. 3.

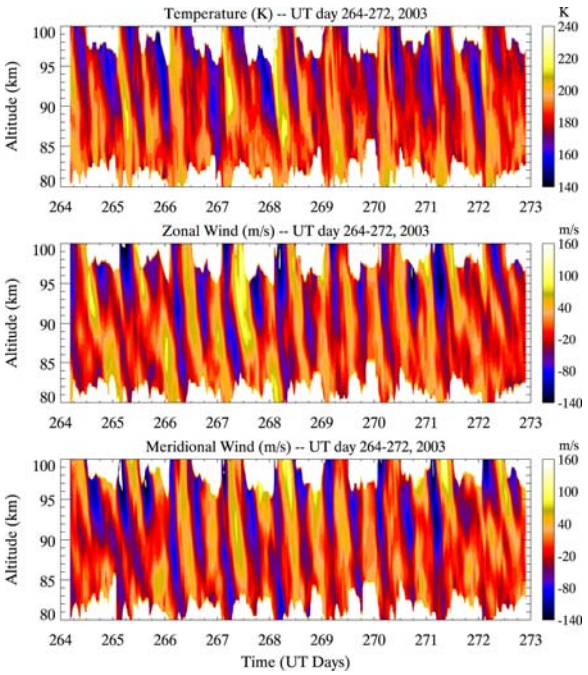

Fig. 3 Continuous TUV contours between day 264 and 272, 2003, with 15/30-min resolution for night/day.

Figure 3 revealed 24-hr and 12-hr period oscillations of solar tide. Without further analysis, it is also clear that semidiurnal tides dominate above 90 km, while diurnal and semidiurnal tides make competing contributions below 90 km. Not so obvious, but it is also quite clear that shorter period oscillations with downward phase progression can be seen intermittently to last many hours, contributing to tidal variability [13]. If we apply a band-pass filter (30 – 120-hr) to these data throughout the 14-day campaign, planetary waves can also be seen. As an example, we show the filtered meridional wind contours in Fig. 4, revealing downward phase progressions of 1.5-day and 3-day waves along with a 5-day trapped wave. Science studies at CSU include concurrent observations with imagers for instability dynamics [14] and other relevant studies summarized by Yuan et al. [15] in this conference.

To illustrate the importance of observation in the arctic, we select a lidar observation during a multiple instrument rocket campaign at ALOMAR in July 2, 2002. Figure 5(a) shows the sodium density measured by the west and east beams, pointing 20^o from Zenith. The sharp decrease in Na density at around 90 km

reflects a very cold mesopause [16]. Below this altitude, the MST radar observed polar mesospheric summer echo (PMSE) and Rayleigh lidar observed noctilucent cloud (NLC) revealed the presence of ice particles that trapped Na atoms on their cold surfaces. In Fig. 5(b), simultaneous lidar temperature profiles and an ionization gauge in a rocket both measure a 40 K temperature decrease within an altitude range of less than 1 km. The accompanying high zonal wind gradient and direction change [16], suggested gravity wave breaking [17]. Though the rocket measurement only lasted a few minutes, lidar observed that these sharp gradients lasted for about 3 hours.

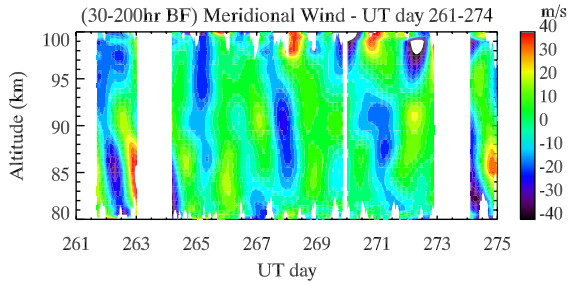

Figure 4 Filtered meridional wind contours, from [14].

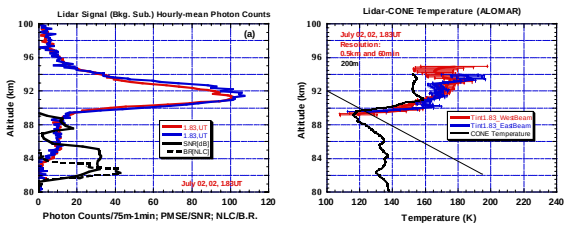

Figure 5 (a). Hourly mean Na density by lidar beams along with simultaneous NLC and PMSE signals, from [16], (b). Hourly mean lidar temperatures centered at the rocket-ionization gauge temperature, from [17].

3. Conclusion and outlook

Over the past 15 years, the narrowband Na lidar has evolved from a proto-type instrument into a robust work horse for observing mesopause region temperature and horizontal wind on 24 hour basis, weather permitting. The new narrowband lidar is heading towards an all-solid-state transmitter system for remote and mobile deployment. In addition to tidal climatology [18], the main scientific interests will continue on studies of tidal variability and of mean state- tide- gravity wave interactions. Taking advantage of large receiving mirrors and/or night time conditions, measurements on gravity wave fluxes with east-west dual beam geometry (for momentum flux) and/or with vertical beam (for heat and constituent fluxes) have begun at ALOMAR and CSU, following the initial measurements at Starfire Optical Range, NM [19].

The work was in part supported by National Aeronautics and Space Administration, under grant NAG5-10076 and National Science Foundation, under grant ATM-00-03171.

4. Referencess

[1]. Gibson, A. J., L. Thomas and S. K. Bhattachacharyya, Laser observations of the ground-state hyperfine structure of sodium and of temperatures in the upper atmosphere, Nature, 281, 131-132, 1979.
[2]. Fricke, K. H., and U. von Zhan, Mesopause temperatures derived from probing the hyperfine structure of the D2 resonance line of sodium by lidar, JASTP, 47, 499-512, 1985.
[3]. She, C. Y. et al., Two-Frequency Lidar Technique for Mesospheric Na Temperature Measurements, Geophys. Res. Lett. 17, 929-932, 1990.
[4]. She, C. Y., and J. R. Yu, Simultaneous three-frequency Na lidar measurements of radial wind and temperature in the mesopause region, Geophys. Res. Lett., 21, 1771-1774, 1994.
[5]. Chen, H. et al., Daytime mesopause temperature measurements using a sodium-vapor dispersive Faraday filter in lidar receiver, Opt. Lett., 21, 1003-1005, 1996.
[6] She, C. Y., and J. R. Yu, Doppler-Free Saturation Fluorescence Spectroscopy of Na Atoms for Atmospheric Applications", Appl. Opt., 34, 1063-1075, 1995.
[7]. Vance, J. D., C.Y. She, and H. Moosmuller, Continuous-wave, all-sol;id-state, single-frequency 400-mW source at 589 nm based on doubly resonant sum-frequency mixing in a monolithic lithum niobate resonator, Appl. Optics 37, 4891-4896, 1998.
[8]. She, C.-Y., On atmospheric lidar performance comparison: from power aperture to power–aperture–mixing ratio–scattering cross-section, Modern Optics, 52, 2723-2729, 2005.
[9]. She, C. Y. et al., Lidar studies of atmospheric dynamics near polar mesopause, EOS, Transactions, American Geophysical Union, 83 (27), P.289 and P.293, 2002.
[10]. Kawahara TD, Gardner CS, Nomura A, Observed temperature structure of the atmosphere above Syowa Station, Antarctica (69 degrees S, 39 degrees E),Jour. Geophys. Res.-ATMOSPHERES 109 (D12): Art. No. D12103 JUN 23 2004.
[11]. Vance, J. D. et al., An all-solid-state transportable narrowband sodium lidar for mesopause region temperature and horizontal wind measurements, the 23rd ILRC proceedings.
[12]. Moosmuller H, Vance JD, Sum frequency generation of continuous-wave sodium D-2 resonance radiation, Opt. Lett., 22, 1135-1137, 1997.
[13]. She, C.Y et al., Tidal perturbations and variability in the mesopause region over Fort Collins, CO (41N, 105W): Continuous multi-day temperature and wind lidar observations, Geophys. Res. Lett., 31, L24111, doi:10.1029/2004GL021165, 2004.
[14]. Li, T. et al., Concurrent OH imager and sodium temperature-wind lidar observation of localized ripples over Northern Colorado, *J. Geophys. Res.* 110, D13110, doi:10.1029/2004JD004885, 2005.
[15]. Yuan, T. et al., The CSU sodium lidar facility: Current observation capability and science, the 23rd ILRC proceedings.
[16]. She, C. Y. et al., Observation of anti-correlation between sodium atoms and PMSE/NLC in summer mesopause at ALOMAR, Norway (69N, 12E), *J. Atmos. Solar-Terres. Phys*. 68, 93-101, 2005.
[17]. Fritts, D. C. et al., Observations of extreme temperature and wind gradients near the summer mesopause during the MaCWAVE/MIDAS rocket campaign, Geophys. Res. Lett., 31, L24S06, doi:10.1029/2003GL019389, 2004.
[18]. Yuan et al., Seasonal variation of diurnal perturbations in mesopause-region temperature, zonal, and meridional winds above Fort Collins, CO (40.6°N, 105°W), *J. Geophys. Res.* 111, D06103, doi:10.1029/2004JD005486, 2006.
[19]. Gardner, C. S., and W. Yang, Measurement of dynamical cooling rate associated with the vertical transport of heat by dissipating gravity waves in the mesopause region at the Starfire Optical Range, New Mexico, J. Geophys. Res., 103, 16,909, 1998.